19th Australasian Fluid Mechanics Conference
Melbourne, Australia
8-11 December 2014

# Experimental Investigation of Flapping Wing Aerodynamics

**M. Scavarelli, N. Wells, T. Wiggins, N. Williams, L. Foster, F. Hampton, and R. Caruso**

Department of Mechanical Engineering
The University of Adelaide, South Australia 5005, Australia

## Abstract

Lift generation of a flapping wing was investigated by varying the frequency and sweep angle (amplitude) of the wing's flapping motion. The wing was attached to a mechanism that altered rotational motion into the desired flapping motion. This setup was connected to an aluminium beam, with accompanying strain gauges, in order to determine the effect of the lift generation on beam strain. The strain readings were then analysed by a data acquisition system (DAQ) and computer, to convert the raw data to lift forces. It was found that the frequency had a non-linear power function relation to the lift, while the amplitude had a reasonably linear relationship to the lift. This showed that controlling a micro air vehicle (MAV) through the use of amplitude control mechanism would allow for an easy lift control method, provided that this mechanism is not overly complicated.

## Background

Flapping wing flight has long been the interest of zoologists and aeronautical engineers alike. In particular, flying insects use unsteady aerodynamics to achieve flight at low Reynolds numbers ($Re \approx 10^2$) by combining the mechanisms of delayed stall, wake capture and rotational circulation [1]. This allows these animals to achieve remarkable manoeuvrability and stability at small scales and low speeds.

The capabilities of flying insects make flapping flight an attractive option for the control and propulsion of micro-air vehicles (MAV). These vehicles have potential applications in military surveillance and reconnaissance, search-and-rescue operations and hazardous environment exploration among others [2]. In such applications, these vehicles are expected to operate in environments where manoeuvrability at low speeds is essential, such as indoors and other confined spaces. Flapping flight is well-suited to this requirement, especially when compared to traditional fixed-wing aircraft which must fly at high speeds to generate sufficient lift. Furthermore, there is evidence to suggest that flapping flight may require low aerodynamic power per unit mass, due to the amalgamation of lift, propulsion and control surfaces. The potential applications of flapping flight have made it a popular research area in recent years.

## Introduction

An honours project currently being conducted at the Department of Mechanical Engineering, University of Adelaide, aims to design and build a flapping-wing MAV. The proposed vehicle uses four wings for lift generation. A control system will be implemented to adjust the lift generated by each wing individually as required to maintain stable flight and conduct manoeuvres. A major component of this project is the design of a flapping mechanism and wing that generates sufficient lift to maintain flight, and allows for the controlled variation of this lift in real-time.

To this end, a flapping mechanism has been developed to convert the rotary motion input by a motor into the flapping motion required to generate lift. This mechanism allows the flapping amplitude and frequency of a wing to be adjusted independently. To complement this wing model, a testing rig was constructed to measure the lift force generated by a single flapping wing in quiescent air. This allowed the lift generated by a single wing to be determined experimentally and expressed as a function of frequency and amplitude. This paper presents the results of this experiment, which will ultimately be used in the control system of the proposed MAV.

## Experimental Apparatus

### Flapping Mechanism

The flapping mechanism is a critical component in the experimental apparatus and ultimately the flapping-wing MAV. In order to mimic insect flapping wing kinematics, the wing must undergo simultaneous sweeping and pitching motions [3]. In addition, the mechanism needs to allow independent control over flapping amplitude and frequency. A computer aided design (CAD) image of the chosen mechanism is provided in figure 1.

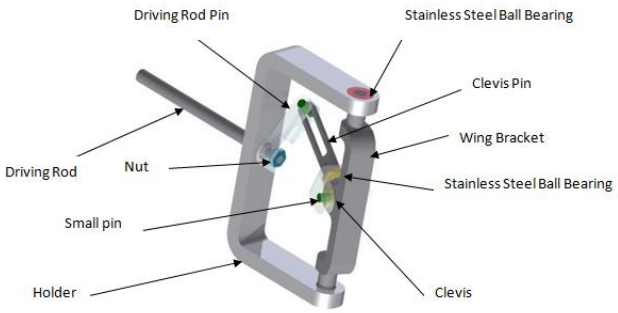


Figure 1. CAD model of the flapping mechanism design. Some components are coloured or partially transparent for clarity.

A motor and drive train assembly produces rotary motion of the driving rod. The motion of the driving rod pin, clevis pin, and clevis convert this rotary motion into oscillatory motion in the wing bracket, which pivots in the horizontal plane about the stainless steel ball bearings (coloured red). The wing root is attached to the wing bracket, which causes the vertically oriented wing to undergo sweeping motion in the horizontal plane. The wing is flexible, and therefore undergoes pitching motion due to the action of inertial and aerodynamic forces throughout the flapping cycle.

In addition to generating flapping motion, the mechanism allows independent control over the flapping amplitude (the total sweep angle of the wing) and the flapping frequency (the number of flaps per second). The flapping amplitude is increased by moving the driving rod in the axial direction towards the wing bracket, and vice versa. This alters the position of the driving rod pin, which changes the angle of the clevis pin to increase the range of wing bracket motion, and thus the flapping amplitude. This mechanism will allow servos to independently adjust the flapping

amplitude of each wing in the final MAV design. Additionally, the flapping frequency is controlled by adjusting the motor speed.

## Wing

A number of design requirements were placed on the wing in order to allow the generation of lift. The wing needed to be lightweight to minimise power input to the motor, flexible to allow pitching motion from the action of inertial and aerodynamic forces, and have a high surface area to maximise the aerodynamic forces and resulting lift generation. The chosen design utilised carbon fibre and styrene stiffeners connected by a thin Mylar film. Carbon fibre stiffeners were included along the leading edge and wing root, while the less rigid styrene stiffeners were included throughout the wing surface. Both stiffener materials were sufficiently flexible to allow pitching motion throughout the flapping cycle. The wing materials were connected using high quality sail repair tape. The wing is approximately 12cm long from root to tip. A schematic diagram of the wing design is included in figure 2.

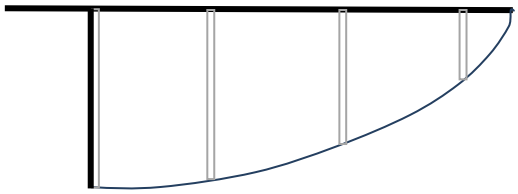

Figure 2. Schematic diagram of the wing design. Carbon fibre stiffeners (black) are included along the leading edge and wing root. Styrene stiffeners (white) are distributed throughout the wing surface. The stiffeners are connected by Mylar film and joined using high quality sail repair tape.

## Testing Rig – Design

The testing rig was designed to measure the lift force generated by a single flapping wing in quiescent air. Given the small mass of the proposed vehicle, it was expected that the maximum lift generated in one wing would be less than 30g. Hence, the testing rig needed to be capable of measuring very small forces generated in the wing. The chosen design was a cantilever beam, fixed to a rigid surface, with strain gauges to measure the strain in the beam, due to the wing lift. A schematic diagram of this configuration is provided in figure 3.

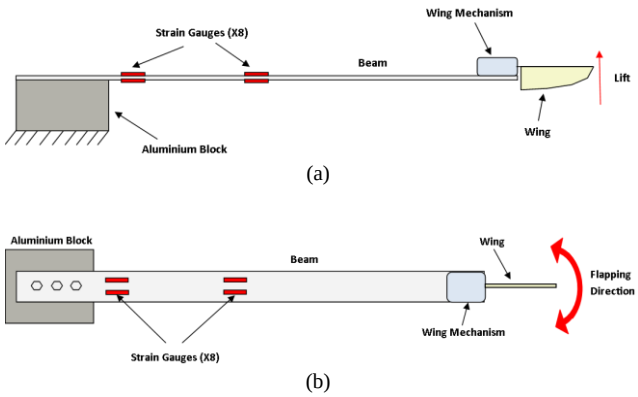


Figure 3. Schematic diagram of the cantilever beam configuration used for the testing rig; (a) side view, (b) plan view. The aluminium block is fixed to a rigid surface. Eight strain gauges are arranged in two Wheatstone bridge configurations to measure beam strain. The component labelled wing mechanism includes the motor, drive train, and flapping mechanism.

In order to reliably measure lift using this design, all load-bearing elements are self-contained within the wing mechanism that is fixed on the end of the beam. As such, this component includes the motor, drive train, and flapping mechanism. The motor is connected to the external power source using lead wires. A CAD image of the wing mechanism assembly on the cantilever beam is provided in figure 4.

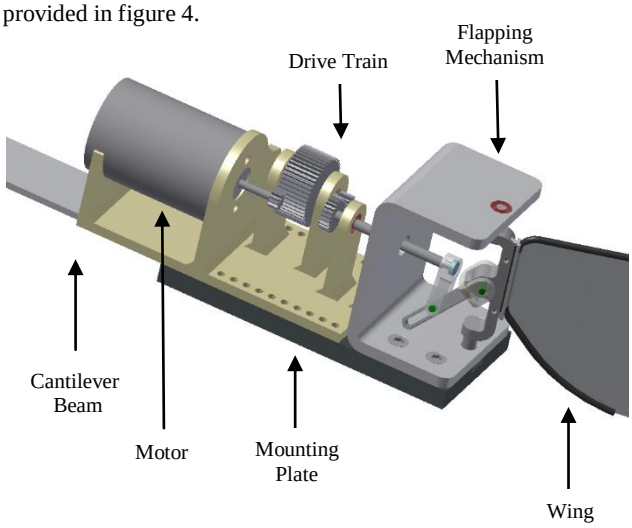


Figure 4. CAD model of the wing mechanism assembly on the cantilever beam. Some components are coloured or partially transparent for clarity.

The strain gauges' sensitivity and beam dimensions allowed a measurement resolution of about 0.2g. Lift force was selected to be measured in grams at the standard gravitational acceleration to simplify the applicability of the results to the weight budget of the final MAV design. These strain gauges were arranged in two Wheatstone bridge formations at two points on the beam. The Wheatstone bridge was selected to reduce noise in the signal, while two Wheatstone bridges were included at different locations to allow both the magnitude and location of the lift force to be determined (the location value was not required for this initial testing). The signal wires were connected to a National Instruments DAQ. A desktop computer then interfaced with the DAQ, and LabView software was used to convert the strain gauge measurements into a lift force in real-time, which was recorded and saved at 50 samples/second. Additionally, a small laser detector and receiver was mounted near the flapping wing, in order to measure the flapping frequency in real time.

## Testing Rig – Calibration

In order to calibrate the testing rig, an equation was derived for the lift force in terms of the material properties and measurable strains. With reference to figure 3, the 'T' represents the thrust generated by the wing Epsilon 2 represents the strain closest to the aluminium block, Epsilon 1 represents the strain mid beam, and all other symbols refer to material properties and geometry of the beam, as shown in equation (1).

$$T = \frac{EI}{by}(\varepsilon_2 - \varepsilon_1) \quad (1)$$

Using theoretical and measured values for the material properties and dimensions respectively was deemed too inaccurate for this application. To compensate for this inaccuracy, the material properties and dimensions were consolidated into a single constant, as shown in equation (2) below.

$$T = C_1(\varepsilon_2 - \varepsilon_1) \quad (2)$$

In order to determine the value of the constant '$C_1$', a known 58.79g weight was placed on the beam and the corresponding strain gauge readings were recorded. Equation (2) was then solved for the constant. This enabled all strains to be converted back into a lift force at the end of the beam. This calibration was

then confirmed with other weights of known masses to ensure accuracy. It should be noted that the position of the weight was not important, as the thrust is determined by the difference between the strains and remains unaffected by force's location when the beam material acts in its linear region.

### Testing Procedure

Testing was conducted in an efficient manner in order to get a large amount of data in the shortest possible time. Data was gathered at a specific amplitude for various frequencies including: 5, 8, 10, 12, 14 and 15Hz. Once these data points were gathered, the wing was stepped up a number of degrees, in order to provide results somewhere around 60, 70, 80 and 90 degree flapping amplitudes. Not all of the measured amplitudes were exactly on these specified numbers, due to a limitation of the testing rig design, which only allowed linear driving rod adjustments to the nearest millimetre.

Once the motor platform had been secured in its desired position, the amplitude of the wing was measured using a fixed protractor on the top of the testing rig. With this part of the setup complete, the strain gauges were calibrated in LabView to eliminate any source of error. The calibration method involved allowing the beam to stabilise so that only noise was read on the output (noise was determined to be all measurements less than 1 micro-strain). Once stable, LabView was told that this was the zero position of the strain gauges, effectively calibrating them at the desired location. With the strain gauges calibrated to zero, the motor was allowed to be powered on. The voltage on the power supply was then slowly ramped up until the desired frequency was detected by the frequency measuring apparatus. Upon achieving the target frequency, measurements of the voltage and current were taken after a few seconds. The wing was allowed to run for at least 10 seconds, with the signal conditioning extension for instrumentation (SCXI) chassis DAQ and computer, logging strain gauge data at 50 samples per second for this time period. This was to ensure that a reasonable average of the lift could be taken, due to the cyclic nature of flapping wing forces. As previously stated, this method allowed for a measurements resolution of about 0.2g, which was deemed acceptable for this analysis. This testing procedure was repeated for all desired amplitudes and frequencies in order to gather the required data.

### Results and Analysis

The gathered data showed interesting trends in flapping wing lift production when altering both frequency and amplitude. It was expected that the lift produced by a flapping wing would be directly proportional to both the square of the frequency and the square of the flapping amplitude from Ellington [4]. The measured vibrations were generally sinusoidal (with fluctuations of about 20% from the average lift), making it relatively easy to take an average value for lift, and draw relationships from there.

#### Frequency Relationships

The comparison between lift and frequency is close to what was expected from a flapping wing. By increasing the overall frequency of the flapping wing, the lift production also showed an increase. The most notable part of this results is the increase appeared to be non-linear for all chosen amplitudes, as shown in figure 5.

From further analysis, using computer technology to perform a least squares regression, it was found the most suitable models for these curves were power functions (apart from the lowest amplitude, which is more susceptible to experimental error and therefore discounted for this purpose). Fluctuations about these trend lines are likely due to measurement errors associated with the recorded frequency and amplitude. The resolution of these values was relatively low but acceptable, at approximately 0.5Hz and 1 degree respectively, which may have affected results. In addition, vibrations of the cantilever beam may have affected the accuracy of the lift measurement, although such vibrations were minor in comparison to the other error sources. The least squares regression power functions ranged from powers of 2 up to 2.5. This lies somewhat inline with other literature stating that the lift should be directly proportional to the frequency squared [4]. The fact that the relationships do not directly agree with other literature is not of great concern as flapping wing aerodynamic equations are generally approximations. The overall knowledge for flapping wing aerodynamics does not perfectly account for all forces, leading to slight variations between each study.

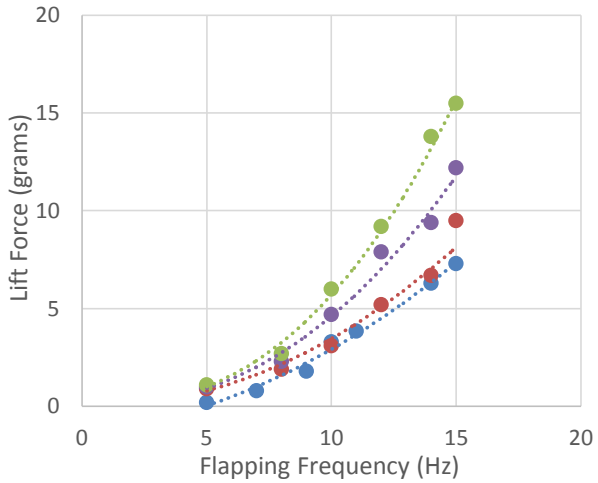


Figure 5. Lift vs. flapping frequency for various amplitudes. Amplitudes include (from top to bottom): 90, 79, 67 and 60 degrees sweep angle.

#### Amplitude Relationships

Similarly to frequency, the amplitude of the flapping motion was adjusted for a specific frequency and then analysed to determine the results. As expected, the lift increased with an overall increasing sweep angle for the wing. However, the relationship between lift and amplitude was more linear as opposed to the frequency relationship which seemed to obey a power function. This was unexpected as it was thought that the amplitude would also obey a power function (to the power of 2) similar to that of frequency. The results can be seen in figure 6 below.

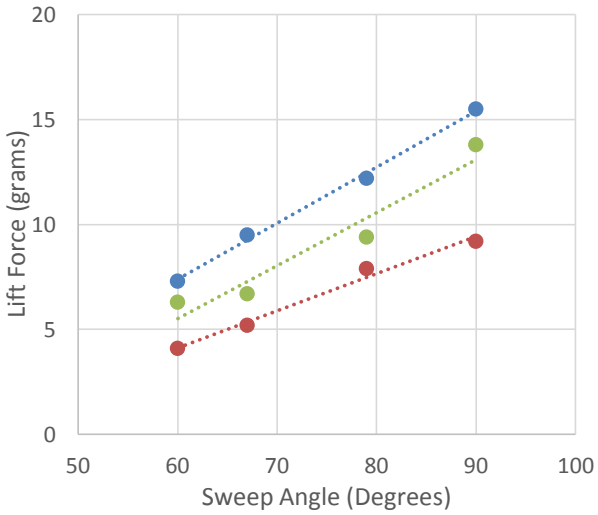


Figure 6. Lift vs. sweep angle (amplitude) for various frequencies. Various frequencies include (from top to bottom): 15, 14 and 12Hz.

By similar computational methods as performed in the frequency varying case, an analysis was conducted into the effect of amplitude on the lift force of a flapping wing. The most appropriate relationships for the sweep angle data appeared to be a series of linear functions. This is different to what is suggested by Shy & Liu [5], which suggests that amplitude and frequency should have a similar effect on the change in lift. This again can be attributed to the approximations related to flapping wing aerodynamics. The discrepancy may have come from a variation in wing design, or general variations in the operation of the wing mechanism. Once again, fluctuations about the trend lines are likely attributed to the resolution of the measured frequency and amplitude. With all things considered, it appears that variations in the sweep angle of a flapping wing produce a reasonably linear change in the overall lift.

## Conclusion

It was found that both frequency and amplitude have a significant effect on the lift generated by a flapping wing. The relationship between frequency and lift was found to obey a power function while the relationship between amplitude and lift was more linear. This information provides a basis for a full micro air vehicle design, in the way that these relationships can be used to balance and control an MAV through the use of lift variation in each wing.

## Acknowledgments

The authors of this paper would like to officially acknowledge Dr. Maziar Arjomandi as the supervisor of the overall project and for his valuable input into this work. Additionally, the authors would also like to acknowledge Mr. Ryan Leknys for his assistance in LabView and strain gauge setup, and Mr. David Betteridge for his input into designing flapping wing mechanisms.

## References

[1] Loh, K., Cook, M. & Thomasson, P., An investigation into the longitudinal dynamics and control of a flapping wing micro air vehicle at hovering flight, *The Aeronautical Journal*, **107**, 2003, 743-753.

[2] Motamed, M. & Yan, J., A reinforcement learning approach to lift generation in flapping MAVs: simulation results, in *Robotics and Automation*, *IEEE International Conference*, 2006, 748-754.

[3] Sun, M. & Tang, J., Unsteady aerodynamic force generation by a model fruit fly wing in flapping motion, *The Journal of Experimental Biology*, **205**, 2002, 55-70.

[4] Ellington C.P., The novel aerodynamics of insect flight: applications to micro-air vehicles, *The Journal of Experimental Biology*, **202**, 1999, 3439-3448.

[5] Shy, W. & Liu, H., Flapping wings and aerodynamic lift: the role of leading-edge vortices, *AIAA Journal*, **45**, 2007, 2817-2819